aspects of a first-order phase transition. Actually, the adsorption isotherm computed with the help of the data obtained possessed the distinctly expressed van der Waals loop. The extension of the system size up to 50 centers leads to the disappearance of the bimodality of the function $P^{(50)}(\rho)$ and consequently all the signs of phase transitions disappear as well.

The dependence of $P^{(B)}(N)$ functions on system size is exhibited more clearly when the periodic boundary conditions are implied (see Figure 3). In this case the distribution of the system per particle has three maxima at $B = 5$. It follows from the form of $P^{(5)}(\rho)$ that at such small sizes one out of the three system states is observed with the greatest probability: with low density, with intermediate density, and with density equal to unity. As in the case of the systems without PBC, the extension of the system size leads to a rather rapid disappearance of the polimodality of $P^{(B)}(\rho)$. At $f = 0.1$, $T^* = 0.434$, $B = 40$ the distribution histogram possesses the shape that is typical for a one-phase system.

Cluster formation taking place in the corresponding thermodynamic system of finite sizes could be the reason for the polymodality of the distribution function of small systems per particle. So if the characteristic size of molecular clusters appearing in infinite systems at a given value of T and P is greater than the migration area that is available for these molecules on the adsorbent surface or it is greater than the simulation box in the computer simulation, then the object under consideration will exhibit all signs of a first-order phase transition, although there is no phase transition in the corresponding infinite system.

The calculations presented in this paper have illustrated the essential dependence on system size of the shape of the distribution of systems per particle in the grand canonical ensemble. The developed method of computing the $P^{(B)}(N)$ function can be used to investigate the behavior of more complicated lattice models as well as for the preliminary estimation of the distribution function of finite-size continuum systems.

Ion Transport in a Gramicidin-like Channel: Dynamics and Mobility

Benoît Roux and Martin Karplus*

Department of Chemistry, Harvard University, Cambridge, Massachusetts 02138 *(Received: July 16, 1990)*

The mobility of water, Na^+, and K^+ has been calculated inside a periodic poly-(L,D)-alanine β-helix, a model for the interior of the gramicidin channel. Because of the different dynamical regimes for the three species (high barrier for Na^+, low barrier for K^+, almost free diffusion for water), different methods are used to calculate the mobilities. By use of activated dynamics and a potential of mean force determined previously (Roux, B.; Karplus, M. *Biophys. J.* **1991**, *59*, 961), the barrier crossing rate of Na^+ ion is determined. The motion of Na^+ at the transition state is controlled by local interactions and collisions with the neighboring carbonyls and the two nearest water molecules. There are significant deviations from transition-state theory; the transmission coefficient is equal to 0.11. The water and K^+ motions are found to be well described by a diffusive model; the motion of K^+ appears to be controlled by the diffusion of water. The time-dependent friction functions of Na^+ and K^+ ions in the periodic β-helix are calculated and analyzed by using a generalized Langevin equation approach. Both Na^+ and K^+ suffer many rapid collisions, and their dynamics is overdamped and noninertial. Thus, the selectivity sequence of ions in the β-helix is *not* influenced strongly by their masses.

Introduction

In the first paper of this series,[1] the potential of mean force of water and Na^+ and K^+ ions was calculated as a function of distance along the axis of a periodic poly-(L,D)-alanine gramicidin-like β-helix. The simplified periodic model permitted the study of the potential of mean force in the absence of end effects and made possible the detection of hysteresis and insufficient equilibration in the calculations. Interest in the free energy profile, a concept essential to modern discussion of rate processes in liquids,[2,3] is justified by its fundamental role in controlling the transport of ions through biological channels.[4-8] The free energy profile, rather than dynamical factors, is thought to be the main factor responsible for the selectivity to monovalent cations.[9-13] Different phenomenological approaches based on a knowledge of the free energy profile, such as classical transition-state theory,[14-16] Nernst-Planck continuum diffusion[17] or Brownian dynamics

(1) Roux, B.; Karplus, M. Ion transport in a gramicidin-like channel: Structure and thermodynamics. *Biophys. J.* **1991**, *59*, 961-981.
(2) Hynes, J. T. The theory of reactions in solutions. In *Theory of Chemical Reaction Dynamics*, Baer, M., Ed.; CRC Press: Boca Raton, FL, 1985; pp 171-235.
(3) Chandler, D. Statistical mechanics of isomerization dynamics in liquids and the transition state approximation. *J. Chem. Phys.* **1978**, *68*, 2959-2970.
(4) Hille, B. *Ionic Channels of Excitable Membranes*; Sinauer: Sunderland, MA, 1984.
(5) Copper, K. E.; Gates, P. Y.; Eisenberg, R. S. Surmounting barriers in ionic channels. *Q. Rev. Biophys.* **1988**, *21*, 331-364.
(6) Copper, K. E.; Gates, P. Y.; Eisenberg, R. S. Diffusion theory and discrete rate constant in ion permeation. *J. Membr. Biol.* **1988**, *106*, 95-105.
(7) Jordan, P. C. Microscopic approach to ion transport through transmembrane channels. The model system gramicidin. *J. Phys. Chem.* **1987**, *91*, 6582-6591.
(8) Chiu, S. W.; Jakobsson, E. Stochastic theory of singly occupied ion channels. II. Effects of access resistance and potential gradient extending into the bath. *Biophys. J.* **1989**, *55*, 147-157.
(9) Eisenman, G.; Horn, R. Ionic selectivity revisited: The role of kinetic and equilibrium processes in ion permeation through channels. *J. Membr. Biol.* **1983**, *76*, 197-225.
(10) Finkelstein, A.; Andersen, O. S. The Gramicidin A Channel: A review of its permeability characteristics with special reference to the single-file aspect of transport. *J. Membr. Biol.* **1981**, *59*, 155-171.
(11) Hladky, S. B.; Haydon, D. A. Ion movements in gramicidin channels. *Curr. Top. Membr. Transp.* **1984**, *21*, 327-372.
(12) Cooper, K. E.; Jakobsson, E.; Wolynes, P. G. The theory of ion transport through membrane channels. *Prog. Biophys. Mol. Biol.* **1985**, *46*, 51-96.
(13) Vertenstein, M.; Ronis, D. Microscopic theory of membrane transport. III. Transport in multiple barrier systems. *J. Chem. Phys.* **1986**, *85*, 1628-1649.
(14) Glasstone, S.; Laidler, K. J.; Eyring, H. *Theory of Rate Processes*; McGraw-Hill: New York, 1941.
(15) Läuger, P. Microscopic calculation of ion-transport rates in membrane channels. *Biophys. Chem.* **1982**, *15*, 89-100.
(16) Läuger, P. Ion transport through pores: A rate theory analysis. *Biochim. Biophys. Acta* **1973**, *311*, 423-441.

0022-3654/91/2095-4856$02.50/0

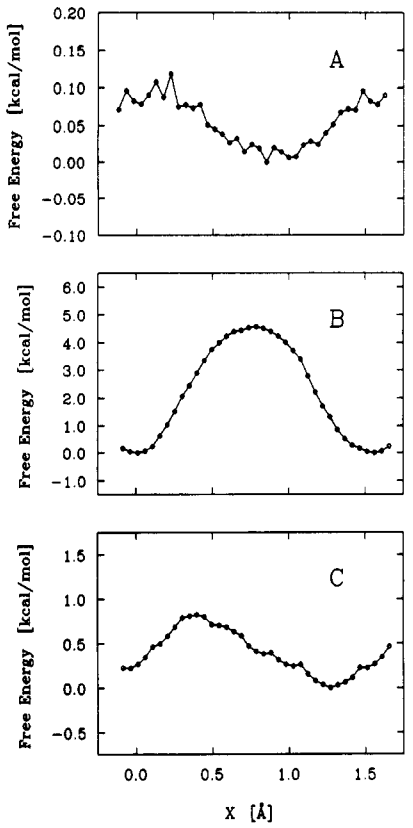

Figure 1. Free energy profiles of water (A), Na^+ (B), and K^+ (C).[1] The zeros of energy correspond to the minima of the profiles. The free energy barriers are 0.1, 4.5, and 1.0 kcal/mol for water, Na^+, and K^+, respectively.

stochastic simulations,[8] have been used to describe ion transport in the gramicidin A channel. To provide a more complete description of the transport through a channel it is necessary also to determine the dissipative and collisional recrossing effects at the transition state, which are neglected in classical transition-state theory,[3] and the non-Markovian inertial dynamical effects, which are neglected by the Nernst–Planck approach.[18] Studies based on a detailed atomic model with realistic interactions are required to elucidate the microscopic nature of ion motions and dynamics inside the gramicidin A channel. Although the ion selectivity is of interest, the differences in the permeabilities to monovalent cations are less than a factor of 3;[11] for instance, the permeabilities of K^+ and Cs^+ relative to Na^+ are 1.47 and 1.55, respectively. Such small differences could be accounted for by changes of only 0.4 kcal/mol in the activation energies, which would be within the uncertainty of present computational methods. However, these differences in the permeabilities could also arise from dynamical factors. In a sense, the question of interest is not the difference in mobility of the various ions but rather why such different ions have such similar mobilities. Thus, in a study of ion permeation based on a detailed atomic model, it is less the absolute transport rate than the analysis of the microscopic factors not directly accessible to experimental measurements that is of interest.

The goal of this paper is to investigate the dynamics of ions and water molecules inside the periodic β-helix model. To study the dynamics associated with the rate of transport, it is necessary to choose computational techniques appropriate for the time scales of the problem under investigation. It has been shown for the periodic β-helix[1] that the activation free energy barriers for water, Na^+, and K^+ are weak (0.2 kcal/mol), strong (4.5 kcal/mol), and moderate (1.0 kcal/mol) relative to k_BT at 300 K, respectively (see Figure 1). Even though both dissipative and activation factors are expected to play a role in the motion of the three species through the β-helix, each one clearly belongs to a different dynamical regime and appropriate computational methods, adapted to the proper time scales, must be chosen to estimate the rate of transport. When the barrier is small or nonexistent, as in the case of water, transport proceeds as a continuous diffusive process controlled by dissipative forces and a description in terms of discrete transitions is not appropriate. Because the free energy profile of water is essentially uniform inside the β-helix, sufficient translational displacement of the water molecules is expected to take place during the time scale of a normal molecular dynamics trajectory to obtain the diffusion constant directly from the mean-square displacement correlation function, as in previous studies of bulk water.[19] For one-dimensional diffusion, the expression is

$$D = \lim_{t\to\infty} \frac{\langle [x(t) - x(0)]^2 \rangle}{2t} \tag{1}$$

where x is the displacement coordinate along the helix axis (in the case of water, the coordinate of the oxygen atom was used). This direct approach is impractical in the case of the Na^+ ion. Because of the relatively large free energy barrier (4.5 kcal/mol), the average time spent in a well is expected to be on the order of $\sim 10^{-8}$ s, and a significant number of transitions would not be expected to take place during the 100 ps of a normal molecular dynamics trajectory. When transport is controlled by a series of equivalent barriers separated by a distance ΔL, as for Na^+, it is appropriate to express the long-time transport in terms of an effective diffusion constant[20]

$$D_{\text{eff}} \simeq k\Delta L^2 \tag{2}$$

where k is the barrier crossing rate, which can be determined by using activated dynamics techniques (see below).[3,21]

The transport of the K^+ ion belongs to an intermediate case, which is more difficult to treat quantitatively. The barrier of 1.0 kcal/mol for the K^+ makes its motion too slow ($\sim 10^{-10}$–10^{-11} s) to be studied directly during a typical molecular dynamics trajectory. However, unlike Na^+, the description in terms of uncorrelated discrete transitions is unrealistic for such a small free energy barrier since a transition rate is not well-defined for an activation barrier on the order of k_BT.[3] An alternative approach is to estimate the effective diffusion constant D_{eff} from the displacement of the K^+ ion in response to a weak external force $\mathcal{F}_{\text{ext}}$,

$$D_{\text{eff}}(t) = \lim_{\mathcal{F}_{\text{ext}}\to 0} \frac{\langle [x(t) - x(0)] \rangle k_BT}{t\mathcal{F}_{\text{ext}}} \tag{3}$$

The average response is less sensitive to statistical uncertainties than the mean-square displacement correlation function of eq 1, which is based on equilibrium fluctuations. Thus, this approach is useful for estimating the transport for an ion with an intermediate activation energy barrier for which there is no well-defined transition rate. By choosing an external force of appropriate magnitude, it is possible to observe significant average displacements. The present calculation is similar in spirit to the subtraction method of Ciccotti and Jacucci[22,23] for determining transport coefficients. Their method relies on initial conformations, taken from an equilibrium trajectory, from which short nonequilibrium

(17) Levitt, D. G. Interpretation of biological channel flux data—Reaction-rate theory versus continuum theory. *Annu. Rev. Biophys. Chem.* **1986**, *15*, 29–57.
(18) McQuarrie, D. A. *Statistical Mechanics*; Harper and Row: New York, 1976.
(19) Stillinger, F. H.; Rahman, A. Molecular dynamics study of liquid water. *J. Chem. Phys.* **1974**, *60*, 1545.
(20) Weaver, D. L. Note on the interpretation of lateral diffusion coefficients. *Biophys. J.* **1982**, *38*, 311–313.
(21) Berne, B. J. Molecular dynamics and monte carlo simulations of rare events. In *Multiple Time Scales*; Academic Press: New York, 1985; pp 419–436.
(22) Kuschick, J.; Berne, B. J. Molecular dynamics methods: Continuous potentials. In *Statistical Mechanics*; Plenum Press: New York, 1976; Part B pp 41–63.
(23) Ciccotti, G.; Jacucci, G. Direct computation of dynamical response by molecular dynamics: The mobility of a charged Lennard-Jones particle. *Phys. Rev. Lett.* **1975**, *35*, 789–792.

trajectories are generated in the presence of a weak external field. The difference between the behavior in the absence and presence of the field (extrapolated to zero field) is then used to evaluate the transport coefficient. Because of the activation barrier present for K^+, too few of the equilibrium trajectories would sample the top of the free energy barrier. Thus, the direct approach used here is expected to converge more rapidly, though it suffers from the fact that finite fields have to be used to obtain meaningful results.

The atomic model, the empirical energy function, and the simulation techniques are described in the Methodology section. The transport rate and the effective diffusion constant of water, Na^+, and K^+ are then calculated. Order of magnitude comparisons are made with experimental estimates of the transport rates through the gramicidin channel. To obtain more insight into the ion motions, they are analyzed in the framework of the generalized Langevin equation.[24] A concluding discussion summarizes our understanding of the periodic system and its relation to the real gramicidin channel.

Methodology

Atomic Model and Potential Function. The β-helix model and the details of the molecular dynamics simulations have been described elsewhere.[1] All heavy atoms and all polar hydrogens (those able to form hydrogen bonds) are included. The aliphatic hydrogens are treated as part of the carbon to which they are attached in an extended atom model. The β-helix is constructed from 17 (L,D)-alanine dipeptide units, 1 cation and 8 water molecules, or no ion and 9 water molecules in the water-filled channel simulation.

The system was treated with periodic boundary conditions to avoid end effects, and a group-by-group based cutoff of 12 Å was applied to all nonbonded interactions. The total length of the system is 26.35 Å, corresponding to 17 L-ala,D-ala helical units with a rise of 1.55 Å per unit. The total number of particles is 229 in the ion–helix simulations and 231 in the water–helix simulation. The helix is oriented along the positive x axis and the 34 alanine residues are numbered from the N terminus to the C terminus; the odd-numbered L-alanine carbonyls point toward the N terminus ($+x$) and the even-numbered D-alanine carbonyls point toward the C terminus ($-x$). The reaction coordinate describing the ion translocation and the diffusion of water molecules is the position of the ion along the x axis relative to the center of mass of the β-helix.[1] The center of mass of the helix was constrained at a constant position along the x axis by using the SHAKE algorithm[25] in all the simulations. The integration time step for the dynamics was 1 fs.

Special care was given to the parametrization of the interaction of the ion with the channel and water. From ab initio calculations with Na^+ interacting with the carbonyl group of the acetamide molecule, it was found that a good description of the interaction must include an attractive ion-induced dipole polarization term and that that ion–carbonyl oxygen repulsion was best represented by a $1/r^8$ core repulsion, softer than the more standard $\sim 1/r^{12}$ repulsion of the Lennard-Jones 6–12 potential.[26] Only the dominant first-order polarization induced by the ion on the peptide was included; i.e., the partial charges of the peptide and the water as well as other induced dipoles do not influence a particular induced dipole. The water–water (TIP3P),[27] peptide–peptide (CHARMM),[28] and water–peptide[29] potential functions have been described elsewhere. All the ion interaction parameters used in the calculation are reported in refs 1 and 26. The calculations with the periodic β-helix system were performed with the CHARMM program,[28] appropriately modified to incorporate the ion–peptide potential.

Computational Details and Simulation Procedure. Water Molecules: Mean-Square Displacement. The mean-square displacement correlation function in eq 1 is calculated by averaging over all possible origins in time t' and over distinct water molecules in the system ($N = 9$); i.e.,

$$\langle [x(t) - x(0)]^2 \rangle = \frac{1}{N} \sum_{n'=1}^{N} \frac{1}{T_{tot}} \int_0^{T_{tot}} [x_{n'}(t' + t) - x_{n'}(t')]^2 \, dt' \tag{4}$$

The one-dimensional diffusion constant was also obtained from the autocorrelation function of the x component of the velocity, $C(t) = \langle v(0)\, v(t) \rangle$, using the Green–Kubo relation[30]

$$D = \int_0^\infty \langle v(0)\, v(t) \rangle \, dt \tag{5}$$

Other correlation functions were calculated for the purpose of analysis. They include the x component nearest-neighbor oxygen velocity correlation functions $C_n(t) = \langle v_1(0)\, v_{1+n}(t) \rangle$, the water dipole autocorrelation function $C_{dd}(t) = \langle \vec{\mu}(0) \cdot \vec{\mu}(t) \rangle$, and the nearest-neighbor oxygen density distribution function

$$\langle \rho_n(x) \rangle = \frac{1}{N} \sum_{n'=1}^{N} \langle \delta(x_{n+n'} - x_{n'} - x) \rangle \tag{6}$$

The velocity autocorrelation function $C(t) = \langle v(0)\, v(t) \rangle$ in eq 5 is a special case of $C_n(t)$ with $n = 0$. The correlation functions were all calculated by using the periodic boundary conditions of the water-filled channel system ($n + N$ is the same as water n) and by averaging over all possible origins in time t'. For example, the nearest-neighbor oxygen velocity correlation functions, $C_n(t)$, is calculated as

$$C_n(t) = \frac{1}{N} \sum_{n'=1}^{N} \frac{1}{T_{tot}} \int_0^{T_{tot}} v_{n+n'}(t') v_{n'}(t' + t) \, dt' \tag{7}$$

The water mean-square displacement and other correlation functions were calculated from a 250-ps molecular dynamics trajectory of the water-filled β-helix without any ions at 300 K.

Na^+ Ion: Activated Dynamics. The forward transition rate in eq 2 is calculated from[3]

$$k = \kappa \frac{\langle v\theta(v) \rangle e^{-\mathcal{W}(x_b)/k_B T}}{\int e^{-\mathcal{W}(x')/k_B T} \, dx'} \tag{8}$$

where κ is the transmission coefficient; x and v are the position and the x component of the velocity of the ion (i.e., along the reaction coordinate x); $\mathcal{W}(x)$ is the potential of mean force; x_b is the position of the barrier; θ is a Heaviside step function and the integral in the denominator is over the "reactant" well along the reaction coordinate ($x_b - \Delta L < x < x_b$). The potential of mean force of the ion $\mathcal{W}(x) = -k_B T \ln \langle \delta(x) \rangle$ had been calculated along the x axis of the β-helix by using free energy simulation techniques, as described in ref 1. It is a function of x alone; all other degrees of freedom, including the y and z coordinates of the ion, have been integrated out. Setting the transmission coefficient equal to one in eq 8 leads to the classical transition state or Eyring rate theory estimate of the rate constant, i.e., $k = \kappa k_{TST}$.[3,14] The transmission coefficient includes the deviation of k from the classical transition-state theory rate k_{TST} due to the dissipative and collisional recrossing effects taking place during the transitions. It is calculated from the reactive flux correlation function from an ensemble of activated dynamics trajectories,[3,21] i.e.,

(24) Berne, B. J.; Pecora, R. *Dynamic Light Scattering*; Wiley-Interscience: New York, 1976.
(25) Gunsteren, W. F.; Berendsen, H. J. C. Algorithms for macromolecular dynamics and constraint dynamics. *Mol. Phys.* **1977**, *34*, 1311–1327.
(26) Roux, B.; Karplus, M. Empirical energy function for cations-peptides interactions. Manuscript in preparation.
(27) Jorgensen, W. L.; Impey, R. W.; Chandrasekhar, J.; Madura, J. D.; Klein, M. L. Comparison of simple potential functions for simulating liquid water. *J. Chem. Phys.* **1983**, *79*, 926–935.
(28) Brooks, B. R.; Bruccoleri, R. E.; Olafson, B. D.; States, D. J.; Swaminathan, S.; Karplus, M. CHARMM: A program for macromolecular energy minimization and dynamics calculations. *J. Comput. Chem.* **1983**, *4*, 187.
(29) Reiher III, W. E.; Karplus, M. Theoretical studies of hydrogen bonding. Manuscript in preparation.
(30) Kubo, R. The fluctuation-dissipation theorem. *Rev. Mod. Phys.* **1966**, *29*, 255–284.

$$\kappa = \lim_{t \gg \tau_{mol}} \langle \theta(x[+t] - x_b) - \theta(x[-t] - x_b) \rangle_{(+)} \quad (9)$$

where the subscript (+) implies that the ensemble is generated with a biased position–velocity distribution function $P^{(+)}(\mathbf{R},\mathbf{V})$ given by

$$P^{(+)}(\mathbf{R},\mathbf{V}) = \frac{v\theta(v)\delta(x - x_b)e^{-\mathcal{H}(\mathbf{R},\mathbf{V})/k_BT}}{\int d\mathbf{R}\, d\mathbf{V}\, v\theta(v)\, \delta(x - x_b)e^{-\mathcal{H}(\mathbf{R},\mathbf{V})/k_BT}} \quad (10)$$

where $\mathcal{H}(\mathbf{R},\mathbf{V}) = U(\mathbf{R}) + K(\mathbf{V})$ is the Hamiltonian and $\mathbf{R}$ and $\mathbf{V}$ represents all the coordinates and velocities of the system. In eq 9 the Heaviside functions θ are evaluated relative to x_b, the position of the barrier, and the time τ_{mol} represents the time scale of molecular dissipative and collisional relaxation taking place at the transition state before the barrier crossing is completed.[3] For the existence of a rate constant the molecular relaxation time τ_{mol} should be much shorter than $1/k$.

The transmission coefficient κ was calculated from the reactive flux correlation function eq 9 by using 100 activated dynamics trajectories with initial conditions from the biased distribution function $P^{(+)}$. The ensemble of 100 initial configurations, distributed as $\delta(x - x_b)e^{-U(\mathbf{R})/k_BT}$, was obtained from a 100-ps molecular dynamics trajectory during which the Na^+ was constrained at the transition state with the SHAKE algorithm[25] (one configuration per picosecond was used). The initial velocity of the ion along the channel axis was sampled from the non-Maxwellian velocity distribution $v\theta(v)e^{-mv^2/2k_BT}$, generated from normal random numbers R distributed between 0 and 1 using

$$v = \left[\frac{-2k_BT}{m} \ln (R)\right]^{1/2} \quad (11)$$

where m is the mass of the ion. All other initial velocities were sampled from a Maxwell distribution at 300 K. With these initial conditions, the trajectories were calculated from 0 to $t = +1$ ps to generate $\theta(x[+t] - x_b)$ and they were then run backwards in time from 0 to −1 ps by inverting the sign of all the initial velocities in the system at $t = 0$ to generate $\theta(x[-t] - x_b)$. Thus, the calculation of the transmission coefficient is computationally equivalent to a single trajectory of 200 ps. Trial calculations with longer trajectories showed that the fate of the crossing events is determined within 0.5 ps or so. This is similar to the behavior found in other simulations of activated processes in liquids.[2] To obtain the rate constant k, the transmission coefficient κ is combined with the transition-state-theory rate k_{TST}[14]

$$k_{TST} = \frac{\langle v\theta(v)\rangle e^{-\mathcal{W}(x_b)/k_BT}}{\int e^{-\mathcal{W}(x')/k_BT}\, dx'} = \nu e^{-\Delta\mathcal{W}^{\ddagger}/k_BT} \quad (12)$$

In eq 12 $\Delta\mathcal{W}^{\ddagger}$ is the activation free energy $[\mathcal{W}(x_b) - \mathcal{W}(x_m)]$ and ν is the well frequency

$$\nu = \left[\frac{k_BT}{2\pi m}\right]^{1/2}\left[\int_{x_b - \Delta L}^{x_b} e^{-[\mathcal{W}(x') - \mathcal{W}(x_m)]/k_BT}\, dx'\right] \quad (13)$$

where x_m is the position of the minimum in $\mathcal{W}(x)$. The frequency ν can be related to the second derivative of the potential of mean force at the bottom of the energy well, $2\pi\nu = [\mathcal{W}''(x_m)/m]^{1/2}$, using a quadratic expansion of $\mathcal{W}(x)$ to approximate the integral in eq 13. The transition-state rate k_{TST} was calculated with eqs 12 and 13. All the quantities relevant to the transition rates are summarized in Table I.

K^+ Ion: Response to External Force. The value of the diffusion constant of K^+ ion was calculated with eq 3 from a 50-ps trajectory in the presence of an external electric field applied to all the particles in the system. The value of the electric field was chosen to correspond to a drop of electric potential of 1000 mV over a distance of 30 Å. Trial calculations to estimate the mobility with an applied potential of 500 mV under the same conditions were unsuccessful because no significant net drift was observed in presence of the weaker force. Although much larger than the usual experimental fields (~100 mV/30 Å), a value of 1000 mV is not as large as it may seem. It represents a force of 0.76 (kcal/mol)/Å on the ion, a small force compared to the rms fluctuations of the force acting on the K^+ ion, which are on the order of 8–9 (kcal/mol)/Å (see Table II).

TABLE I: Transition Rate of Na^+ and K^+

ion	properties	values
Na^+	activation energy, $\Delta\mathcal{W}^{\ddagger}$	4.5 kcal/mol
	well frequency, ν	4.0 ps^{-1}
	classical transition rate, k_{TST}	2.1×10^9 s^{-1}
	transmission coeff, κ	0.11
	transition rate $k = \kappa k_{TST}$	2.3×10^8 s^{-1}
	barrier frequency, ω_b	112 cm^{-1}, or 3.4 ps^{-1}
	static friction const, ξ	15.0 (ps-kcal/mol)/Å^2
	Kramers transmission coeff	0.08
	Grote–Hynes transmission coeff	0.10
K^+	activation energy, $\Delta\mathcal{W}^{\ddagger}$	1.0 kcal/mol
	effective[a] transition rate, k	2.4×10^{10} s^{-1}
	barrier frequency, ω_b	44 cm^{-1}, or 1.3 ps^{-1}
	$\langle e^{+\mathcal{W}/k_BT}\rangle\langle e^{-\mathcal{W}/k_BT}\rangle$	2.88
	static friction const, ξ	3.6 (ps-kcal/mol)/Å^2

[a] Effective transition rate k defined as in eq 2, $D_{Na}/\Delta L^2$, with D_{Na} from Table III and $\Delta L = 1.55$ Å.

TABLE II: Time-Dependent Friction $\xi(t)$

ion	environment	initial value, (kcal/mol)/Å^2	$t_{1/2}$,[a] ps	ξ,[b] (ps-kcal/mol)/Å^2
Na^+	β-helix			
	$\xi(t)$	225	0.025	15.0
	$\xi ww(t)$	154	0.020	4.6
	$\xi cc(t)$	49	0.056	5.3
	$\xi cw(t) + \xi wc(t)$	20	0.146	5.1
	bulk[c]			
	$\xi(t)$	166	0.05	9.2
	bulk[d]			4.5
K^+	β-helix			
	$\xi(t)$	125	0.025	3.6
	$\xi ww(t)$	107	0.024	2.4
	$\xi cc(t)$	22	0.054	1.2
	$\xi cw(t) + \xi wc(t)$	−4.2	0.062	0.0
	bulk[d]			3.0

[a] The time, $t_{1/2}$, at half-amplitude $\xi(t_{1/2})$ is $\xi(0)/2$. [b] Static friction $\xi = \tilde{\xi}(s = 0)$ in eq 22. [c] From molecular dynamics in water.[52] [d] Friction extracted using $\xi = k_BT/D$ from the experimental diffusion constant in bulk water.[4]

Generalized Langevin Equation Analysis. To gain further insight into the dynamics of Na^+ and K^+ ions inside the β-helix their dynamics is analyzed in terms of a generalized Langevin equation[24,31-33]

$$m\dot{v} = -\mathcal{W}'(x) - \int_0^t \xi(t-t')v(t')\, dt' + f(t) \quad (14)$$

where $\xi(t)$ is a time-dependent friction function and $f(t)$ is a Gaussian random force with zero average, obeying the fluctuation–dissipation theorem[30]

$$\xi(t) = \frac{\langle f(t)\, f(0)\rangle}{k_BT} \quad (15)$$

Although no formal derivation of eq 14 is available in the general case, it is a useful tool to analyze the dynamics in dense liquids.[34,35]

(31) Zwanzig, R. W. Time-correlation functions and transport coefficients in statistical mechanics. *Annu. Rev. Phys. Chem.* **1965**, *16*, 67–102.
(32) Adelman, S. A. Generalized Langevin equation and many-body problems in chemical dynamics. *Adv. Chem. Phys.* **1980**, *44*, 143–253.
(33) Brooks III, C. L.; Adelman, S. A. Dynamics of liquid state chemical reactions: R-dependent correlation functions for I+I in CCl_4. *J. Chem. Phys.* **1982**, *76*, 1007–1023.
(34) Grote, R. F.; Hynes, J. T. The stable states picture of chemical reactions. II. Rate constants for condensed and gas phase reaction models. *J. Chem. Phys.* **1980**, *73*, 2715–2732.
(35) Straub, J.; Berne, B. Molecular dynamics study of an isomerizing diatomic in a Lennard-Jones fluid. *J. Chem. Phys.* **1988**, *89*, 4833–4847.

It assumes that all variables other than the reaction coordinate x are at equilibrium at all times (since x moves in the potential of mean force $\mathcal{W}(x)$). The deviations of the instantaneous force from its mean value are taken into account through the time-dependent friction function $\xi(t)$ and the random Gaussian force $f(t)$. To employ eq 14, it is necessary to estimate the time-dependent friction $\xi(t)$ from the microscopic model. The random force $f(t)$ in eq 14 can be identified with $\delta F(t)$, the deviation of the instantaneous force relative to the average force acting on the ion constrained at a position along the channel axis; the average force is $\langle F(x)\rangle = -\mathcal{W}'(x)$. This approximate relation can be used to extract the time-dependent friction from a molecular dynamics trajectory,[36,37] i.e.,

$$\xi(t) = \frac{\langle \delta F(t)\, \delta F(0)\rangle}{k_B T} \tag{16}$$

where $\delta F(t) = F(t) - \langle F\rangle$. Based on eq 16 the fluctuating force can be decomposed in water–water, channel–channel, and water–channel cross contributions

$$\xi(t) = \frac{1}{k_B T}\langle [\delta F_w(t) + \delta F_c(t)][\delta F_w(0) + \delta F_c(0)]\rangle$$
$$= \xi_{ww}(t) + \xi_{cc}(t) + \xi_{cw}(t) + \xi_{wc}(t) \tag{17}$$

with

$$\xi_{ww}(t) = \frac{\langle \delta F_w(t)\, \delta F_w(0)\rangle}{k_B T} \tag{18}$$

and the others defined similarly (notice that $\xi_{cw}(t)$ and $\xi_{wc}(t)$ are equivalent only for $t = 0$). The autocorrelation function of the force acting on the Na^+ ion along the x axis was computed for two values of x. The first value corresponds to the transition state $x = x_b$. For this purpose, the 100-ps trajectory used to generate the initial configurations for the activated dynamics was analyzed. Another 100-ps trajectory was calculated with the Na^+ ion constrained at the position $x = x_b + 0.2$ Å to extract the second correlation function; at this position, the free energy value is $\sim k_B T$ below the barrier height. The autocorrelation function of the force acting on the K^+ ion along the x axis was computed from a 100-ps trajectory with the ion constrained at the top of the free energy barrier. The contribution of water and channel forces to $\xi(t)$ were calculated by using eq 17 for the Na^+ and K^+ ions.

The absolute error of the time-dependent friction $\xi(t)$ is on the order of[38]

$$\text{error} \simeq \pm\xi(0)\left[\frac{2\tau}{T_{tot}}\right]^{1/2} \tag{19}$$

where T_{tot} is the simulation time. In eq 19 $\xi(0)$ is the initial value of the correlation function and τ represents a molecular time scale which is on the order of 0.1 ps in the present case. Because the fluctuations in the instantaneous force acting on the ion, $\langle \delta F^2\rangle$, are very large, it is difficult to obtain a very accurate time-dependent friction beyond 1 or 2 ps with a 100-ps trajectory. From eq 19, the error is on the order of ±5 (kcal/mol)/Å^2. The various contributions to the static friction were calculated from $\xi(t)$ by truncating the time integration at 1.25 ps. Changing the truncation from 1.0 to 1.5 ps did not affect the result significantly; the variation is on the order of 10%. The results are summarized in Table II.

To analyze the transport rate in the framework of the generalized Langevin equation it is necessary to consider the limiting cases of high-energy activation barriers (Na^+) and overdamped

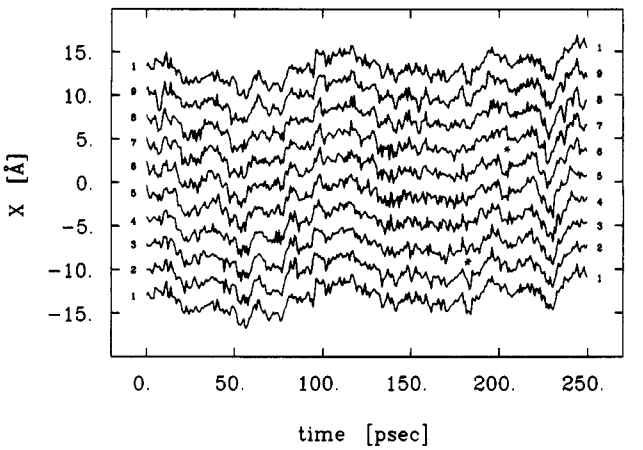

Figure 2. Time series of the displacement of the water molecules along the β-helix axis during the molecular dynamics trajectory. The waters are numbered from 1 to 9 from the bottom to the top (the trajectory of water 1 is repeated at the top). Defects in the water chain are seen to occur for water 2 and 3, and water 6 and 7 around 200 ps (marked with a *).

Markovian diffusion (K^+) because there is no general solution to eq 14 in a periodic potential.[39] When a transition rate is well-defined, as in the case of Na^+, the transmission coefficient can be estimated by the Grote–Hynes theory of barrier crossing,[34]

$$\kappa_{GH} = \lambda_r/\omega_b \tag{20}$$

where ω_b is the frequency corresponding to the curvature of the potential of mean force at the top of the barrier, i.e., $\omega_b^2 = -\mathcal{W}''(x_b)/m$, with $\mathcal{W}''(x_b) < 0$, and λ_r is the "reactive" frequency, obtained from the equation

$$(\omega_b^2 - \lambda_r^2) = \lambda_r \tilde{\xi}(\lambda_r)/m \tag{21}$$

where $\tilde{\xi}(s)$ is the Laplace transform of the time-dependent friction

$$\tilde{\xi}(s) = \int_0^\infty \xi(t) e^{-st}\, dt \tag{22}$$

Non-Markovian behavior and memory effects become negligible when the time-dependent friction $\xi(t)$ is large and decays rapidly compared to other time scales in the system, such as the frequency ω_b of the inverted energy barrier at the transition state. In the high-friction Markovian regime, the dynamics is determined by the static friction constant, denoted by $\xi \equiv \tilde{\xi}(s = 0)$ in eq 22, and the transmission coefficient is given by the Kramers limit[40]

$$\kappa_K = m\omega_b/\xi \tag{23}$$

The Kramers limit is recovered by the Grote–Hynes theory in eq 20 if $\tilde{\xi}(\lambda_r)$ is replaced by $\tilde{\xi}(0)$ and the inertial term λ_r^2, (arising from the Laplace transform of the $m\dot{v}$ term in eq 14, is neglected in eq 21.[34] In the case of K^+, the activation energy is small and a transition-state-rate description is not appropriate. If non-Markovian effects are negligible, the effective diffusion constant can be estimated as the average one-dimensional resistance[41-43]

$$D_{eff} = \frac{k_B T}{\xi}\langle e^{-\mathcal{W}/k_B T}\rangle^{-1}\langle e^{+\mathcal{W}/k_B T}\rangle^{-1} \tag{24}$$

where the brackets $\langle ...\rangle$ represent a spatial average over the diffusion space x and ξ is the static friction.

(36) Bergsma, J. P.; Reimers, J. R.; Wilson, K. R.; Hynes, J. T. Molecular dynamics of the A+BC reaction in rare gas solution. *J. Chem. Phys.* **1986**, *85*, 5625–5643.
(37) Berne, B. J.; Tuckerman, M.; Straub, J.; Bug, A. L. R. Dynamic friction on rigid and flexible bonds. *J. Chem. Phys.*, in press.
(38) Zwanzig, R. W.; Ailawadi, N. K. Statistical error due to finite time averaging in computer experiments. *Phys. Rev.* **1969**, *182*, 280–283.
(39) Risken, H. *The Fokker-Planck Equation. Methods and Applications*; Springer-Verlag: Berlin, 1984.
(40) Kramers, H. A. Brownian motion in a field of force and the diffusion model of chemical reactions. *Physica* **1940**, *7*, 284–304.
(41) Lifson, S.; Jackson, J. L. On the self-diffusion of ions in a polyelectrolyte solution. *J. Phys. Chem.* **1962**, *36*, 2410–2414.
(42) Zwanzig, R. W. Diffusion in a rough potential. *Proc. Natl. Acad. Sci. U.S.A.* **1988**, *85*, 2029–2030.
(43) Golden, K.; Goldstein, S.; Lebowitz, J. L. Classical transport in modulated structures. *Phys. Rev. Lett.* **1985**, *55*, 2629–2632.

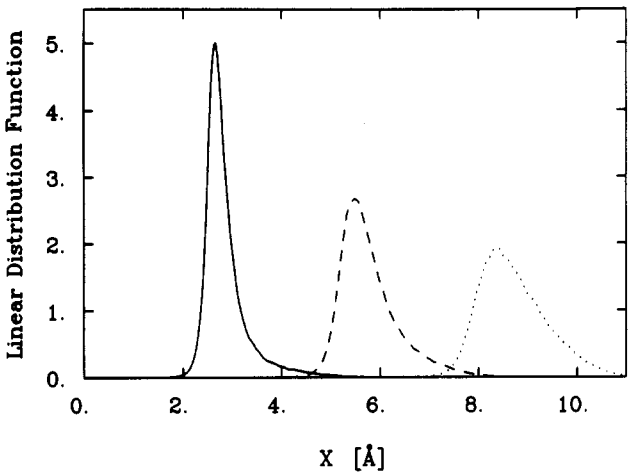

Figure 3. Water oxygen first (solid line), second (dashed), and third (dotted) neighbor linear density distribution function in the β-helix averaged over the nine waters in the helix (calculated from eq 6). The nearest-neighbor peak occurs at 2.58 Å with rms fluctuations of 0.4 Å.

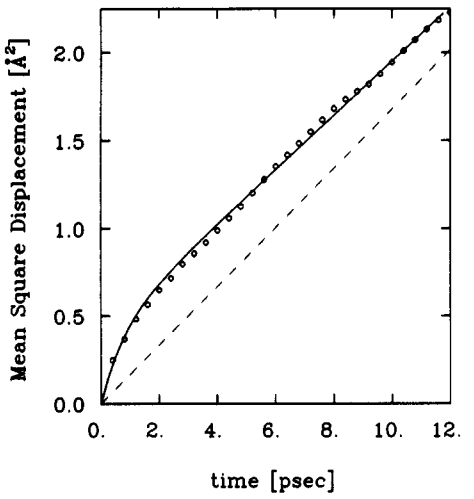

Figure 4. Mean-square displacement correlation function (circles) along the axis of the β-helix for the diffusion of water as calculated from eq 4. The fit using the two time scales model for the mean-square displacement, eq 26, is shown (solid line) with values of $\delta x^2 = 0.206$ Å^2, $\tau = 0.8$ ps, and $D = 0.077$ Å^2/ps.

Results and Analysis

Water Diffusion. At the end of the equilibration period the nine water molecules were found to be oriented in a linear hydrogen-bonded array (with the oxygens directed toward the N terminus of the β-helix). This conformational result is similar to what has been observed in previous simulations of the gramicidin channel.[44-46] After 116 ps a transition occurred and the orientation of all the water molecules was inverted. No significant difference in the overall water motion was observed in the two segments of the trajectory, so the statistical averages were calculated by using the whole 250-ps trajectory. The translational movement of the nine water molecules along the helix axis, shown in Figure 2, is clearly highly correlated, although defects in the water chain are seen to occur for water 2 and 3, and water 6 and 7 around 200 ps. The linear one-dimensional distribution functions around a tagged water molecule calculated with eq 6 (Figure 3) show that the water chain has a well-defined structure with small fluctuations. The first peak in the distribution function is located

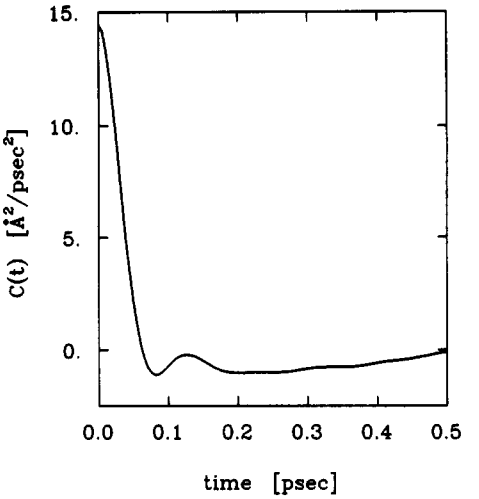

Figure 5. Water oxygen velocity autocorrelation function along the axis of the β-helix averaged over the nine waters in the helix.

at $x = 2.58$ Å. The average relative distance fluctuations along x are on the order of 0.4 Å for the nearest neighbors and 0.6 Å for the second neighbors. The time development of the mean-square displacement correlation function and the negative values of the water velocity autocorrelation function indicates that the water molecules are trapped in an effective cage for short times (see below).

The water oxygen mean-square displacement correlation function is shown in Figure 4. Prior to averaging over the nine waters, the absolute error of the mean-square displacement as a function of time is on the order of[47]

$$\text{error} \simeq \pm Dt\left[\frac{t}{T_{\text{tot}}}\right]^{1/2} \tag{25}$$

where T_{tot} is the simulation time. Averaging over the nine waters does not reduce the error significantly because their motion is highly correlated in this one-dimensional system. Equation 25 indicates that it is more accurate to extract the diffusion constant from the mean-square displacement at relatively short time compared to the total length of the simulation since the relative error increases with time. The diffusion coefficient was extracted by least-squares fitting the mean-square displacement correlation function between 0 and 12 ps with a functional form corresponding to a bounded librational motion with mean-square fluctuations $\langle \delta x^2 \rangle$ occurring on a short time scale τ_f and a long-time (asymptotic) diffusion motion with a diffusion constant D

$$\langle [x(t) - x(0)]^2 \rangle = 2\langle \delta x^2 \rangle (1 - e^{t/\tau_f}) + 2Dt \tag{26}$$

The fitted curve shown in Figure 4 corresponds to values of $D = 0.077$ Å^2/ps, $\langle \delta x^2 \rangle = 0.206$ Å^2, and $\tau_f = 0.8$ ps. Integration of the velocity autocorrelation function shown in Figure 5 from 0 to 1.5 ps (beyond 1.5 ps the correlation function is inaccurate) gives an estimate of D of 0.084 Å^2/ps from eq 5. This is in good agreement with the estimate from the mean-square displacement correlation function.

From the fit it appears that rapid oscillations in a well take place over a time of 0.8 ps, after which the long-time asymptotic diffusion takes over and the displacement increases linearly with time. Assuming that the bounded librational motion corresponds to the movements inside a square well of width ΔL along the x axis, the mean-square fluctuations $\langle \delta x^2 \rangle$ are

$$\langle \delta x^2 \rangle = \frac{1}{\Delta L}\int_{-\Delta L/2}^{+\Delta L/2} x^2\, dx = \frac{\Delta L^2}{12} \tag{27}$$

(44) Mackay, D. H.; Berens, P. H.; Wilson, K. R. Structure and dynamics of ion transport through Gramicidin A. *Biophys. J.* **1983**, *46*, 229–248.
(45) Chiu, S. W.; Subramaniam, S.; Jakobsson, E.; McCammon, J. A. Water and polypeptide conformation in the gramicidin channel. *Biophys. J.* **1989**, *56*, 253–261.
(46) Roux, B.; Karplus, M. The dynamics of water in the gramicidin channel. Manuscript in preparation.
(47) Lee, S.; Karplus, M. Brownian dynamics simulation: Statistical error of correlation functions. *J. Chem. Phys.* **1984**, *81*, 6106–6118.

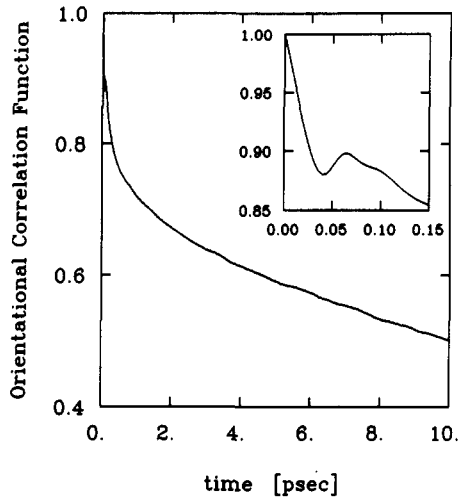

Figure 6. Water dipole autocorrelation function in the β-helix averaged over the nine waters in the helix.

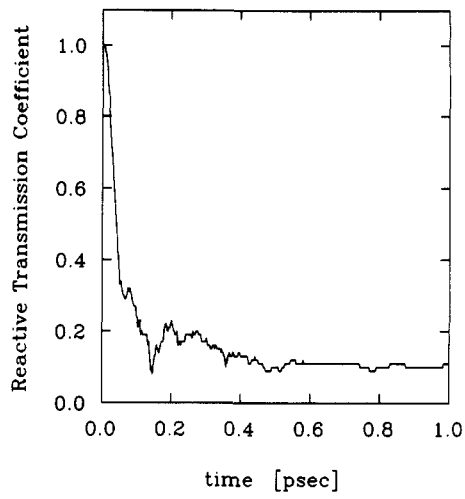

Figure 8. Reactive flux correlation function computed from eq 8. The function decays to a value of 0.11 in less than 1 ps.

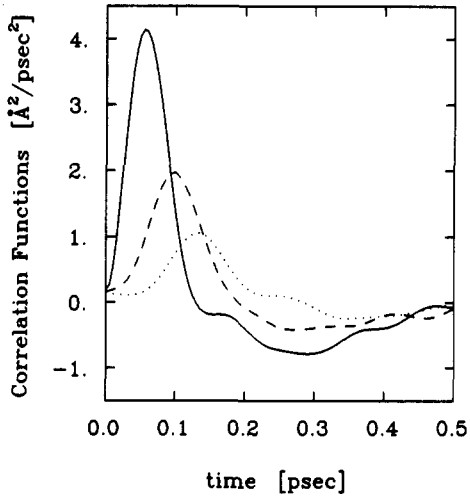

Figure 7. Water oxygen first (solid line), second (dashed line), and third (dotted line) neighbors velocity–velocity correlation functions in the β-helix averaged over the nine waters. The maximum occurs at t = 0.06, 0.10, and 0.13 ps for the first, second, and third neighbors, respectively.

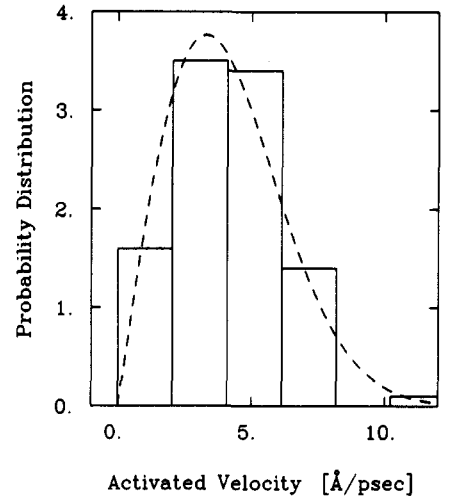

Figure 9. Non-Maxwellian distribution of initial activated velocity generated with eq 10 and assigned to Na^+ for the 100 activated dynamics trajectories to calculate the transmission coefficient in the β-helix. The dashed line represents the biased activated velocity probability density.

From the fitted value of $\langle \delta x^2 \rangle$ (0.206 Å^2) a length of 1.5 Å can be extracted from the simulation, in close agreement with the width of the shallow free energy minimum observed in Figure 1. Thus, in the β-helix, the waters have rapid motions on the time scale of 0.8 ps bounded to a length of 1.5 Å. This is consistent with the negative value of the velocity autocorrelation function between 0.05 and 0.5 ps. Rapid motions are also indicated by the dipole autocorrelation function shown in Figure 6.

The very rapid motions are due to the caging effects by the nearest-neighbor water molecules in the β-helix. Effects of the nearest-neighbor collisions are also apparent in the cross-particle velocity–velocity correlation functions $C_n(t)$ shown in Figure 7. The velocities of the water molecules along the helix axis are highly correlated. The correlation functions reach a maximum value around 0.5–0.1 ps, indicating that momentum is transmitted rapidly to distant neighbors due to the hydrogen-bonded chain. However, the maximum correlation with the third neighbor C_3 is only on the order of 1 Å^2/ps^2, much smaller in magnitude than the mean-square fluctuations of the velocity ($C(0)$ = 15 Å^2/ps^2) to which it should be compared (see Figure 7).

It may be possible that the finite size of the system and the periodic boundary conditions have magnified the orientational correlations in this one-dimensional system due to the long-range dipole–dipole water interactions. However, the dipole autocorrelation function, $C_{dd}(t)$, shown in Figure 6 decays to a value of 0.5 in about 10 ps corresponding to an angular cone of approximately 60° which indicates the presence of significant fluctuations. In fact, the short-time behavior of the orientational correlation function $C_{dd}(t)$ is very similar to that found in bulk water simulations.[48]

Na^+ Motion. The quantities relevant to the barrier crossing rate of Na^+ are summarized in Table I. The reactive flux correlation function, shown in Figure 8, decays rapidly to plateau at a value of 0.11 in less than 0.4 ps. Combining the transition-state-theory result k_{TST} = 2.1 × 10^9 s^{-1} calculated with eq 12, with the transmission coefficient κ = 0.11, we obtain a barrier crossing rate of k = 2.3 × 10^8 s^{-1}. The sampling of the reactive velocity is shown in Figure 9; it is a good representation of the biased velocity distribution function in eqs 10 and 11. Typical example of the four types of activated trajectories, both reactive and nonreactive, are shown in Figure 10. In accord with the rapid decay of the reactive flux correlation function, the fate of the trajectories is determined in 0.5 ps or less. Comparison of the instantaneous forces acting on Na^+ during a reactive and a nonreactive activated dynamics trajectories shows that the channel forces appear to be directly responsible for the recrossing of the nonreactive trajectory. During the successful crossing, shown in Figure 11, the water forces oscillate rapidly and are predominant while the channel forces have moderate amplitude. During the failed crossing, shown in Figure 12, the channel forces are much larger while the water forces have similar amplitudes than during

(48) Rossky, P. J.; Karplus, M. Solvation. A molecular dynamics study of a dipeptide in water. *J. Am. Chem. Soc.* **1979**, *101*, 1913–1937.

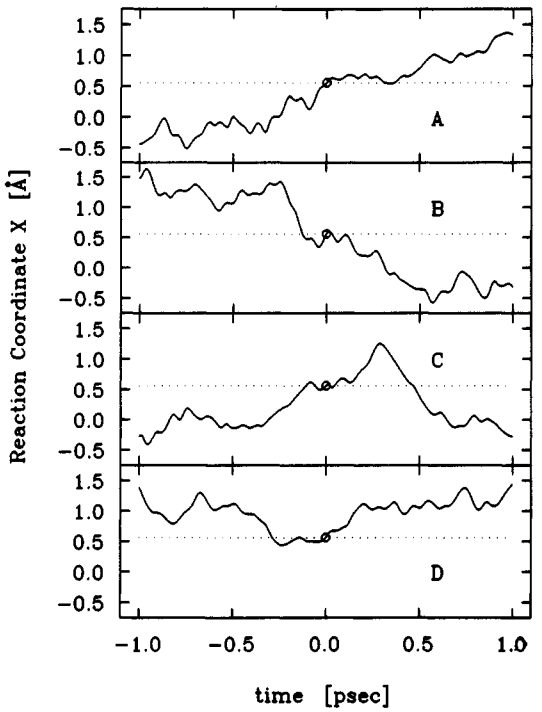

Figure 10. Samples of typical activated trajectories of Na^+ ion. The fate of the crossing event is decided within 1 ps. Among the 100 activated trajectories, there were (A) 26 forward crossing reactive trajectories (reactant to product); (B) 15 backward trajectories (product to reactant); (C) 14 recrossing trajectories (reactant to reactant); and (D) 45 recrossing trajectories (product to product). The transmission coefficient κ is calculated from the *net* number of reactive trajectories by using eq 9, which in the limit $t = 1.0$ ps $\gg \tau_{mol}$ comes out to be $0.11 = (26 - 15)/100$.

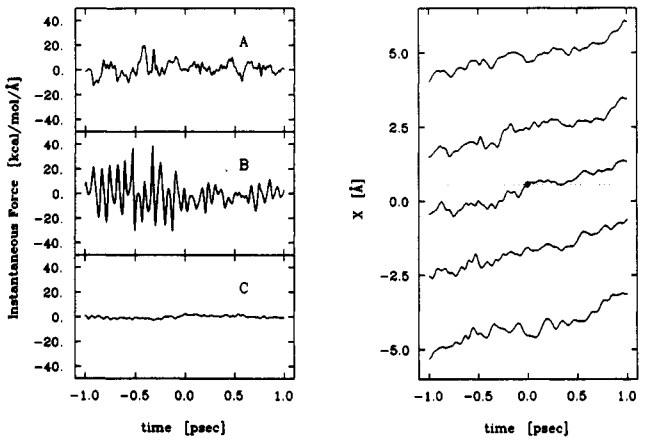

Figure 11. The instantaneous forces acting on Na^+ ion during the reactive trajectory shown in Figure 10A. The forces exerted by the channel (A), the two nearest water molecules (B), and the water molecules other than the two nearest ones (C) are shown on the left. The displacement along the x axis of the ion and the four nearest water molecules is shown as a function of time on the right; the circle indicates the initial position of the ion at the transition state. The motion of the ion is primarily correlated with the two nearest water molecules and the carbonyl forces are not dominant.

the reactive trajectory. The nearest water molecules remain in close contact with the Na^+ ion during both the reactive and nonreactive trajectories. It is clear that the permeation process does not proceed by a vacancy diffusion mechanism as has been suggested.[11,49]

To further analysize the failed crossings, we examine the local structure during the barrier-crossing events. In Figure 13 the initial positions of the Na^+ in the (y,z) plane, corresponding to

(49) Läuger, P.; Stephan, W.; Frehland, E. Fluctuations of barrier structure in ionic channels. *Biochim. Biophys. Acta* **1980**, *602*, 167–180.

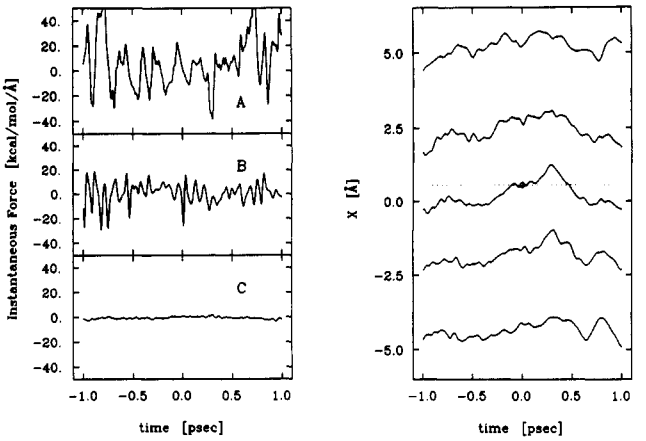

Figure 12. The instantaneous forces acting on Na^+ ion during the nonreactive trajectory shown in Figure 10C. The forces exerted by the channel (A), the two nearest water molecules (B), and the water molecules other than the two nearest ones (C) are shown on the left. The displacement along the x axis of the ion and the four nearest water molecules is shown as a function of time on the right; the circle indicates the initial position of the ion at the transition state. The motion of the ion is correlated with the two nearest two water molecules but the dominant forces causing the recrossing arise primarily from the nearest carbonyl oxygens.

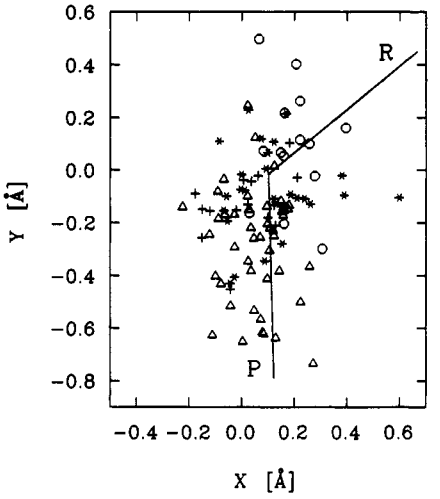

Figure 13. Initial location of the activated dynamics trajectories for Na^+ in the y,z cross section of the channel; the channel axis is perpendicular to the figure plane and is pointing toward the page. The 100 activated dynamics trajectories are distributed as follows: (+) 26 forward crossing reactive trajectories (reactant to product); (*) 15 backward trajectories (product to reactant); (O) 14 recrossing trajectories (reactant to reactant); and (Δ) 45 recrossing trajectories (product to product). The solid line was obtained from energy minimization of the helix,[1] in presence of Na^+ and indicates an "ideal" trajectory to go from the "reactant" to the "product" free energy well.

the channel cross section at the transition state, are plotted. These determine their relation relative to the average carbonyl cage structure around the ion. To obtain Figure 13, the initial configurations used in the 100 activated dynamics trajectories were calculated in a local reference frame to remove the transverse fluctuations of the helix (these fluctuations are on the order of 0.6 Å). The coordinates of the cage atoms are reoriented for each configuration to minimize the root-mean-square displacement from the initial structure. This method has been used previously to analyze the solvation structure around the ion in the binding site and the fluctuations at the transition state.[1] The coordinates of the molecular dynamics at the transition state were reoriented relative to a reference transition-state structure obtained from energy minimization of the helix.[1] Reference reactant and product structures obtained with the same method are also shown in Figure 13. A solid line, obtained by simply connecting the position of the ion in the three structures with straight lines, indicates a

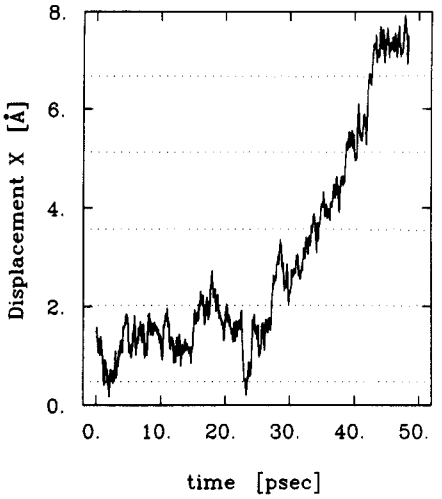

Figure 14. Trajectory of K^+ ion in the presence of an electric potential gradient of 1000 mV in 30 Å or equivalently a force of 0.76 (kcal/mol)/Å. The dotted line indicates the position of the minima in the potential of mean force of K^+ in the periodic β-helix (see Figure 1).

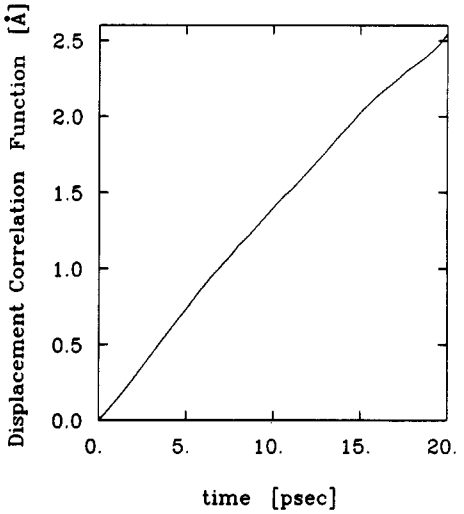

Figure 15. Displacement correlation function of K^+ in the presence of an external force.

fictitious "ideal" trajectory that goes from the reactant to the product free energy well. The four different types of activated trajectories are indicated in the figure by separate symbols. A significant correlation is found between the initial position of the Na^+ relative to local carbonyl cage and the ultimate fate of the trajectory. Most reactant-to-reactant trajectories lie on the upper part of the plot, near the reactant region, and most product-to-product trajectories lie at the bottom of the plot, near the product region. The majority of reactive trajectories are found at the center of the cross section. This shows clearly that the initial position of the Na^+ relative to the nearest carbonyls dominates the crossing events. Similar influence of the initial positions of the ion on the barrier crossings was observed in stochastic simulations of Na^+ in a gramicidin-like model.[13]

K^+ Motion. The displacement of K^+ ion along the helix axis as a function of time under the influence of an external force of 0.75 (kcal/mol)/Å is shown in Figure 14. The resulting displacement correlation function (Figure 15) corresponds to a calculated diffusion constant of 9.7×10^{-2} Å^2/ps using eq 3. The absence of temporary pauses in the energy wells during the trajectory of the K^+ ion, indicated with dashed lines in Figure 14, may indicate that the value obtained for K^+ is an overestimate of the true diffusion constant. This could be due to the magnitude of the applied field. That the value is an overestimate is indicated by an independent estimate of the diffusion constant of K^+ (see below). The response to an external force technique was used

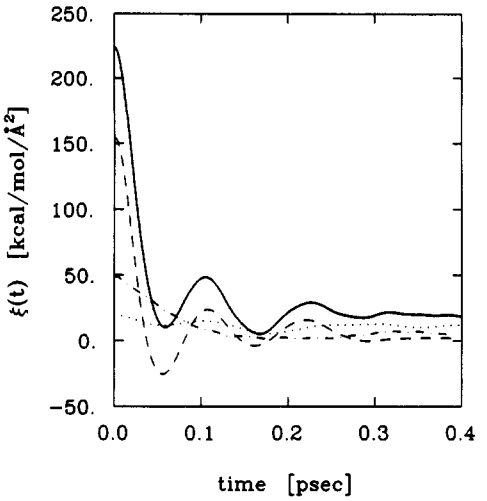

Figure 16. Decomposition of $\xi(t)$ the time-dependent friction of Na^+ ion calculated at the transition state (solid line). The water–water contribution $\xi_{ww}(t)$ (dashed line), the channel–channel $\xi_{cc}(t)$ (dash-dotted line), and the water–channel cross terms $[\xi_{cw}(t) + \xi_{wc}(t)]$ (dotted line) are also shown.

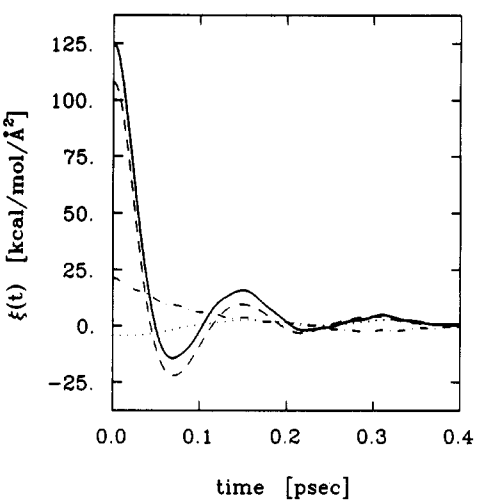

Figure 17. Time-dependent friction function $\xi(t)$ acting on K^+ ion (solid line) at the free energy maximum observed in Figure 1. The water–water contribution $\xi_{ww}(t)$ (dashed line), the channel–channel $\xi_{cc}(t)$ (dash-dotted line), and the water–channel cross terms $[\xi_{cw}(t) + \xi_{wc}(t)]$ (dotted line) are also shown.

previously by Fisher and Brickmann to estimate the mobility of ions in a simplified gramicidin-like helix, even though they extracted the mobility directly from the absolute displacement by least-squares fitting instead of using the correlation function approach in eq 3 and Figure 15.[50] Comparison of Figures 14 and 15 shows that the correlation function is computationally superior.

Time-Dependent Friction and Generalized Langevin Equation. To further our understanding of the dynamical factors influencing the rate of transport of ions in the β-helix, the time-dependent friction along on Na^+ and K^+ is calculated at the top of the free energy barrier and decomposed into the water–water, channel–channel, and water–channel cross coupling contributions (eqs 17 and 18). The decompositions are shown in Figures 16 and 17 and their characteristic features are summarized in Table II. The time-dependent friction functions of the two ions are very similar in form and decay rapidly on a time scale of about 0.1 ps, and then more slowly with oscillations over 1 ps. The dominant short-time contributions arise from the solvent; both the channel and the channel–water cross terms are much smaller. The initial amplitude of the time-dependent friction is smaller by about a

(50) Brickmann, J.; Fisher, W. Entropy effects on the ion diffusion rate in transmembrane protein channels. *Biophys. Chem.* **1983**, *17*, 245–256.

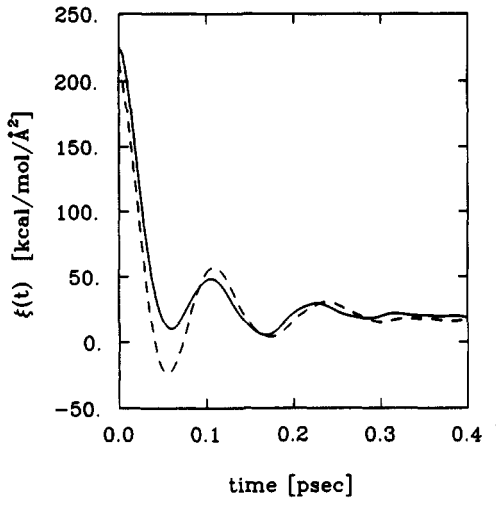

Figure 18. Time-dependent friction of Na^+ ion calculated at the top of the barrier (transition state) (solid line), displaced by 0.2 Å from the top of the barrier (dashed line).

factor of 2 for K^+ than for Na^+. Because K^+ is a larger ion the fluctuating collisional forces $\xi(0) = \langle \delta F^2 \rangle / k_B T$ are weaker. Thus, in the β-helix the net friction acting on Na^+ is larger than for K^+; i.e., both the static friction and the initial amplitude of $\xi(t)$ are larger for the smaller ion. This effect is often described phenomenologically in term of dielectric friction,[4,51,65] which leads to an inverse relation between the ion size and the magnitude of the initial value $\xi(0)$.

The magnitude and the decay time of the time-dependent friction of the Na^+ ion in the β-helix are qualitatively similar to the friction function calculated for the Na^+ ion in water from molecular dynamics.[52] An important difference is the negative excursions around 0.05 ps, shown by the time-dependent friction function of Na^+ and K^+ in the β-helix, a feature not observed in molecular dynamics of Na^+ in water[52] or for other solutes in bulk liquids.[35] This suggests that, at short times, the forces acting on Na^+ and K^+ ions are characteristic of a viscoelastic material; i.e., on a short time scale the ions are caged in a harmonic well (see Figures 16 and 17). The decomposition of the time-dependent friction function reveals that this feature arises from the water–water force–force fluctuation, ξ_{ww}, contribution to $\xi(t)$, which corresponds to an underdamped oscillation with a period of about 0.12 ps. The channel contribution $\xi_{cc}(t)$, which has a smaller initial value than the water contribution, decays monotonically. The net contribution of the water forces to the static friction is larger in the case of Na^+ than K^+, in part due to the larger initial value of the time-dependent friction. The static friction for K^+ is mainly due to the water forces while this constitutes only one-third of the total in the case of Na^+. The water–water, channel–channel, and water–channel cross couplings contribute equally to the total static friction acting on Na^+. The importance of the water–channel cross-coupling contributions suggests that the local ion–water–carbonyl interactions are significant. The instantaneous force acting on Na^+ during the activated trajectories shown in Figures 11 and 12, and the dependence of the fate of the crossing events on the initial configuration in the cross section of the helix shown in Figure 13, are further indications that barrier crossings of Na^+ are controlled by localized interactions. The water–channel couplings are much smaller for the K^+ ion and the water–water force fluctuations constitute most of the total static friction. This is in accord with the fact that the hydrated Na^+ complex in the β-helix is surrounded by a tighter carbonyl oxygen cage than K^+ and that both water and the channel contribute significantly to the potential of mean force for Na^+, by contrast with K^+ where the potential of mean force was determined by water forces only.[1]

The effect of the finite response of the time-dependent friction on the dynamics of the crossing events, the so-called dynamical memory effects,[2] can be described in terms of the generalized Langevin equation.[31,24] Figure 18 shows the time-dependent friction acting on Na^+ at the transition state and displaced by 0.2 Å from the transition state. The distance of 0.2 Å corresponds approximately to a variation of $k_B T$ in the free energy; i.e., it is in the range of the thermal fluctuations at the transition state. Although the time-dependent friction function of Na^+ varies somewhat as a function of the reaction coordinate x in the neighborhood of the transition state, the qualitative and even quantitative features are conserved. Thus eq 14, which assumes that $\xi(t)$ is independent of position in the transition-state region, is a good approximation for the ion dynamics. Vertenstein and Ronis have stressed the importance of the variation of the diffusion coefficient inside the channel.[13] The dependence of the recrossings on the initial position of Na^+ in the (y,z) plane observed in Figure 13 is indicative of similar variations of the friction in the channel cross section. However, the dominant effect controlling the barrier crossing rate appears to be the potential of mean force and the net influence of variations in the friction seems to be small.

The curvature of the free energy barrier $\mathcal{W}''(x_b)$ shown in Figure 1 for Na^+ ion corresponds to a relatively high frequency ω_b (112 cm^{-1}). This implies that the barrier crossing of Na^+ takes place on a time scale which does not allow complete relaxation of the other degrees of freedom in the system; the important libration channel frequencies are in the range 75–150 cm^{-1}.[53] In contrast, the free energy profile of K^+ ion in Figure 1 is much more uniform and corresponds to a lower barrier frequency (for K^+, ω_b is 44 cm^{-1}). Thus the transport of K^+ ion is expected to be controlled by the low-frequency limit of the friction function, and less likely to be sensitive to non-Markovian dynamical effects.

Within the generalized Langevin equation, the transmission coefficient of Na^+ can be obtained by solving the Grote–Hynes eqs 20 and 21 for the barrier crossing[34] with the microscopically calculated time-dependent friction $\xi(t)$. The reactive frequency λ_r is calculated to be 0.34 ps^{-1} corresponding to a transmission coefficient of 0.10, in good agreement with the activated dynamics value of 0.11. The high-friction Markovian limit, eq 23, yields a slightly smaller transmission coefficient of 0.07, indicating that the motion of Na^+ ion is sensitive to non-Markovian dynamical effects due to the finite response time of the time-dependent friction $\xi(t)$ and the narrow barrier. Evaluation of the diffusion constant of K^+ ion from eq 24 gives a value of 4.0×10^{-2} Å²/ps, while the applied field method (eq 3) gives 9.7×10^{-2} Å²/ps. As discussed above, the applied field method may have overestimated the diffusion of K^+ but the agreement within a factor of 2 suggests that eq 24 with the full static friction in the denominator is appropriate for K^+.

The value of the effective diffusion constant of the K^+ ion is very similar to the value found for the water molecules in the periodic β-helix ($D_{H_2O} = 8.4 \times 10^{-2}$ Å²/ps). It is likely that the dissipative factors that affect the mobility of water molecules in the gramicidin channel will strongly influence the overall mobility of K^+ and larger ions as well. This suggests that slow dissipative processes can provide a mechanism that could slow down water and K^+ transport while leaving the mobility of Na^+ unaffected. A low-frequency damping, even though it can reduce the mobility of K^+ ion considerably, has little influence on the barrier crossing of Na^+ ion. Because the dynamics at the top of the barrier is mostly controlled by high-frequency fluctuations, the transmission coefficient of Na^+ ion remains insensitive to the full static friction.

In the actual simulations, the difference is small (i.e., κ is 0.07 with the static friction and 0.11 with the time-dependent friction). This is due to the fact that the reactive frequency corresponds to a relatively long relaxation time scale λ_r^{-1} of 2.94 ps, compared with the very rapid decay time of the time-dependent friction so that $\tilde{\xi}(\lambda_r) \simeq \tilde{\xi}(0)$. It is possible to use the Grote–Hynes theory

(51) Zwanzig, R. W. Dielectric friction on a moving ion II. Revised theory. *J. Chem. Phys.* **1970**, *52*, 3625–3628.
(52) Wilson, M. A.; Pohorille, A.; Pratt, L. R. Molecular Dynamics test of the Brownian description of Na^+ motion in water. *J. Chem. Phys.* **1985**, *83*, 5832–5836.
(53) Roux, B.; Karplus, M. The normal modes of the Gramicidin A dimer channel. *Biophys. J.* **1988**, *53*, 297–309.

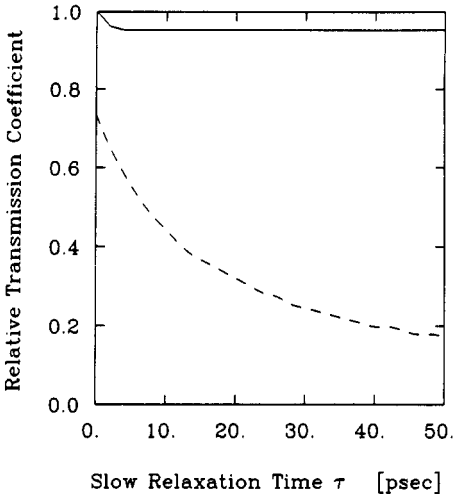

Figure 19. Effect of a slow decaying dissipative process on the transport rate of Na^+ relative to the β-helix calculation. Using eq 27 a slowly decaying exponential tail $\xi_{slow}(t)$ was added to the calculated time-dependent friction calculated from molecular dynamics and displayed in Figure 16. The relative transmission coefficient calculated by using the Grote–Hynes theory of barrier crossings with eq 19 (solid line) and the static friction limit (dashed line).

of barrier crossing[34] to examine the influence of slower relaxation times on the barrier crossing of Na^+ ion in the β-helix. A modified time-dependent friction was constructed by adding a slow decaying exponential tail

$$\xi_{slow}(t) = \frac{\langle \delta F_{slow}^2 \rangle}{k_B T} e^{-t/\tau} \qquad (28)$$

to the time-dependent friction obtained from the molecular dynamics simulation with the Na^+ ion. The weak initial amplitude of the exponential tail $\langle \delta F_{slow}^2 \rangle$ is chosen to be 0.6 (kcal/(mol Å))^2; the latter is calculated from the mean-square force fluctuation arising from the water molecules that are not in direct contact with the ion in the simulation. The transmission coefficient was calculated with eqs 20 and 21 for values of the relaxation time τ varying from 1 to 50 ps. The Kramers limit of the transmission coefficient was also calculated for comparison. The results are shown in Figure 19. Even though a value of the relaxation time τ equal to 50 ps produces an increase of 50 (ps-kcal/mol)/Å^2 in the static friction, Figure 19 shows that the effect of a low-frequency friction on the transmission coefficient of Na^+ is negligible due to non-Markovian dynamical effects. The full static friction does not act on the barrier crossing because the sharp barrier in the potential of mean force of Na^+ corresponds to a high-frequency relative to the response of the time-dependent friction. In contrast with Na^+, the motion of K^+ ion is sensitive to the full static friction in the channel because its potential of mean force ion is flat. According to eq 24 the increase of ξ due to the low-frequency friction of the form used in eq 28 would reduce the diffusion of K^+ by a factor of 15 of its original value. Finally, it should be stressed that the different masses of Na^+ and K^+ play a negligible role in the transport rate in the β-helix. Both Na^+ and K^+ suffer many collisions on a time-scale of 0.5 ps so that the velocity is relaxed rapidly and their dynamics is in the diffusive limit. This is in disagreement with arguments that the selectivity sequence is related to inertial effects (i.e. to the mass).[54,55]

Comparison with Experimental Estimates

Comparison of the present results with experimental values should be made with caution since many of the features of the full gramicidin channel are not included in the periodic β-helix system. At best the periodic β-helix model is a valid description for the interior of the pore. Although there is no direct way to measure the transport rates inside the β-helix it is of interest to consider the available data and compare orders of magnitude. With very simplified models (i.e., with no complex multiple-occupancy effects), the permeability of water, Na^+, and K^+ can be expressed solely in terms of an effective one-dimensional diffusion constant D, the length of the pore L, and its cross-sectional area S. The value of the effective water diffusion constant in the gramicidin channel was extracted from the measured diffusive water permeability P_w by using the expression[56]

$$P_w = SD_w/L \qquad (29)$$

The value of the effective Na^+ diffusion constant was extracted from the maximum single-channel conductance Λ_{max} measured under saturating concentration of permeating ion by using the expression[17]

$$\Lambda_{max} = e^2 D_{ion}/k_B T L^2 \qquad (30)$$

The choice of the microscopic parameters for the channel length L and cross section S is somewhat arbitrary due to the lack of detailed knowledge about the permeation mechanism. The expression for P_w is derived by assuming that the diffusion of the water molecules is rapid in the bulk and limited only by translocation through the channel. Thus, the length L in eq 29 should correspond to the region of the channel that represents the rate-limiting step for permeation. The expression for Λ_{max} is derived under the assumption that no more than one ion can simultaneously occupy the gramicidin channel.[17] This implies that the length L of the pore in eq 30 should correspond to the region of the channel that can contain at most one ion. From the model used for the fully solvated dimer channel, a value of 23 Å for the channel length L and (2.8 Å)^2 for the cross-sectional area is estimated.[46,57] With these values for L and S in eqs 29 and 30 the effective diffusion constants of the gramicidin channel for

TABLE III: Diffusion Constants

species	diffusion const, Å^2/ps	references
H_2O	7.7×10^{-2}	β-helix (MD)[a]
	8.4×10^{-2}	β-helix (MD)[b]
	2.5×10^{-3}	GA channel (MD)[46]
	4.4×10^{-3}	GA channel (exp)[c]
	2.1×10^{-1}	bulk (exp)[4]
	3.2×10^{-1}	bulk TIP3P model (MD)[27]
Na^+	5.5×10^{-4}	β-helix (MD)[d]
	9.4×10^{-4}	GA channel (exp)[e]
	5.8×10^{-2}	GA-like helix (MD)[62]
	2.0×10^{-2}	GA-like channel (BD)[8]
	1.3×10^{-1}	in bulk water (exp)[4]
	4.0×10^{-2}	in bulk water (MD)[52]
K^+	9.7×10^{-2}	β-helix (MD)[f]
	5.7×10^{-2}	β-helix (MD)[g]
	1.8×10^{-3}	GA channel (exp)[h]
	9.0×10^{-2}	GA-like helix (MD)[50]
	2.8×10^{-1}	in bulk water (exp)[4]
	2.8×10^{-1}	in bulk water (MD)[63]

[a] From the mean-square displacement eq 1. [b] From the integral of the velocity autocorrelation function eq 5. [c] Extracted from the experimental diffusional water permeability $P_w = 1.82 \times 10^{-15}$ cm^3/s,[10] using eq 29 with $L = 23$ Å and $S = 7.84$ Å^2. [d] From the transition rate $D = k\Delta L^2$, eq 2. [e] Extracted from the experimental maximum Na^+ conductance $\Lambda_{max} = 14.6$ pmho,[10] using eq 30 with $L = 23$ Å. [f] From the response to an external force, eq 3. [g] From the average resistance path, eq 24. [h] Extracted from the experimental maximal conductance of Na^+,[10] assuming that the Λ_{max} of K^+ is about twice the Λ_{max} of Na^+.[64]

(54) Polymeropoulos, E. E.; Brickmann, J. Molecular dynamics of ion transport through transmembrane model channels. *Annu. Rev. Biophys. Chem.* **1985**, *14*, 315–330.
(55) Schroeder, H.; Brickmann, J.; Fisher, W. Cation transport through biological transmembrane channels. Theoretical study of mass dependent anomalies in the diffusion constant. *Mol. Phys.* **1983**, *49*, 973–979.
(56) Dani, J. A.; Levitt, D. Water transport and ion-water interaction in the gramicidin channel. *Biophys. J.* **1981**, *35*, 501–508.
(57) Roux, B.; Karplus, M. Ion transport in the gramicidin channel: Free energy profile in the right-handed dimer. Manuscript in preparation.

water, Na^+, and K^+ estimated from experiments are given in Table III. A variety of calculated values for water, Na^+, and K^+, including the present results (labeled as β-helix), are also given.

Several factors may limit the comparison between the present simulation of a periodic helix and the experiments. For example, the assumption used to derive eq 30, that the gramicidin channel can be occupied by at most one ion at a time, is probably valid for Na^+ but more uncertain for K^+.[10] Moreover, it has been observed that the maximal conductance of Na^+ and K^+ ions depends on the composition of the lipid membrane; the maximal conductance of Na^+ ion through the gramicidin A channel measured in phosphatidylethanolamine (PE) membranes is 14.6 pS,[10,58] about a factor of 2 smaller than the value measured in glycerylmonooleate (GMO) membranes (27 pS).[11] Such discrepancies indicate that, even under saturating conditions, the rate of ion transport is affected by factors other than the translocation through the channel. If the rate-limiting steps of water or ion passage through the gramicidin channel are located at the entrance or exit, the diffusion constant in the β-helix calculated with eq 30, neglecting the ends effects, may be expected to be larger than the experimental estimate. There is also some uncertainty about the experimental estimate of the diffusional permeability of water. Dani and Levitt reported a value of 6.6×10^{-15} cm^3/s,[56] larger than the value of 1.82×10^{-15} cm^3/s reported by Andersen and Finkelstein.[10]

The estimated water diffusion constant in the β-helix is about 20 times larger than the experimental estimate. The discrepancy could be due in part to the inaccuracy of the microscopic model or of the potential function. The diffusion of the TIP3P water model in bulk calcualted from molecular dynamics simulations is also faster than the experimental value,[27] but only by a factor of 1.5. This suggests that the differences between the periodic β-helix and the full gramicidin channel are responsible for the difference. The hydrogen-bonded water chain observed in the β-helix is more ordered than the water in molecular dynamics simulation of the fully solvated left-handed head-to-head GA dimer.[45,46] The mobility of the water molecules varies significantly in the dimer channel and rotational motions occur on widely different time scales.[46] A slower diffusion and orientational relaxation was observed at the entrance of the channel caused by the local distortion of the β-helix structure at the end of the peptide chain. Such orientational disorder, defects, gaps, and large density fluctuations in the water chain inside the channel are not present in the periodic β-helix. Because the value of the diffusion constant in the β-helix is significantly larger than the experimental estimate, the present calculation indicates that such factors are responsible for the slow water diffusion through the gramicidin channel. This is confirmed by simulation result for water in the full gramicidin channel which yields a diffusion constant in agreement with experiment.[46]

The calculated diffusion constant of Na^+ ion appears to be in reasonable agreement with the experimental estimate. However, since effects other than the translocation inside the helix have been neglected, the apparent agreement with the experimental estimate might indicate that the calculated effective diffusion constant is too small. Nevertheless, the results show that the local interactions in the β-helix per se during the translocation of Na^+ give rise to significant activation barriers that could account for the observed diffusion rate.

The calculated transport rate of K^+ is, as in the case of water, about 30 times larger than the experimental estimates. The origin of the discrepancy could be in the inaccuracies of the microscopic model or factors that are absent in eqs 29 and 30 such as a large energy barrier at the entrance and multiple occupancy of the pore. The large difference in the calculated transport rate of Na^+ and K^+ is due to the potentials of mean force of Na^+ and K^+; i.e., Na^+ has a barrier of 4.5 kcal/mol and K^+ of 1.0 kcal/mol. To obtain agreement with experiment, the free energy of activation for K^+ would have to be increased by 2.0–2.5 kcal/mol. The empirical energy function used for the present calculations were derived from high-level ab initio calculations.[26] Even though there is some uncertainty on the absolute strength of the cation–peptide interaction, the ion size extracted from the ion–carbonyl distance of closest approach is probably determined very accurately. Free energy perturbation calculations indicated that the relative potential of mean force of an ion in the channel is not very sensitive to the absolute interaction energy with the helix and depends mostly on the ion size.[1] The K^+ ion needs to be smaller by 0.2 Å to obtain a change of 2 kcal/mol, a variation in the ion size which seems unacceptable from the ab initio calculations. Thus, error in the parametrization of the Na^+ or K^+ ion model is unlikely to be the source of the incorrect relative diffusion constant. Even though the absolute transport rates for water and K^+ are much larger than the experimental estimates, the ratio D_w/D_K is 2.4 for the experimental estimates and is 1.5 for the calculated values. This suggests that both are sensitive to similar factors, neglected in the periodic β-helix model. It is likely that the rate-determining step for water and K^+ involves the helix and effects due to the ethanolamine tail and at the intermonomer junction.[46] A molecular dynamics simulation of the full solvated dimer channel indicates that the mobility of the water molecules is sensitive to the carbonyl tilting disorder at the channel ends. Experimental channel models without the ethanolamine tail and models that are continuous through the membrane would be of great interest in this regard.

Concluding Discussion

The transport rate of water, Na^+, and K^+ was estimated in a gramicidin-like β-helix model for the interior of the gramicidin channel and the nature of their dynamics was investigated. The movements of water molecules and K^+ are essentially diffusion controlled. The transport of K^+ is slower than that of water molecules due to the dissipative contribution from channel forces and to the modulations of the potential of mean force, which gives rise to a small activation energy. The motion of Na^+ is activated in character and it is appropriate to describe the translocation process in terms of a transition rate. However, the value of the transmission coefficient corresponds to moderately strong friction along the reaction coordinate[2] ($\kappa = 0.1$) and indicates that the motion of Na^+ is significantly more diffusive in character than is pictured in classical transition-state theory. In fact the motion of Na^+ is very close to the Kramers limiting value. Classical transition state theory does not provide a valid picture of the ion motion across the energy barrier since high frequency dissipative forces play an important dynamical role during the barrier crossing; it overestimates the transport rate by one order of magnitude for Na^+. This observation contradicts the statement that the transmission coefficient is near unity for ions in the gramicidin channel.[59] The failure of Eyring rate theory ($\kappa \ll 1.0$) is in part due to the choice for the reaction coordinate. The correlation between the reactive trajectories and the initial position of the ion in the cross section of the channel is one indication that the value of the transmission coefficient is influenced by structural, nondissipative, effects. Different choices for the reaction coordinate could incorporate the motion of the ion in the cross section of the channel and might yield a transmission coefficient closer to 1. Such curvilinear reaction coordinates for ion transport have been suggested and discussed previously.[13,60] However, the value of the molecular transition rate $k = \kappa k_{TST}$ as given by eq 8 is *independent* of the choice of reaction coordinate.[3,61]

(58) Andersen, O. S.; Procopio, J. Ion movement through gramicidin A channels. *Acta Physiol. Suppl.* **1980**, *481*, 27–35.

(59) Åqvist, J.; Warshel, A. Energetics of ion permeation through membrane channels. *Biophys. J.* **1989**, *56*, 171–182.

(60) Schroder, H. Rate theory analysis of ion-selectivity in membrane channels with elastically bound ligands. *Eur. Biophys. J.* **1985**, *12*, 129–142.

(61) Northrup, S. H.; Pear, M. R.; Lee, C. Y.; McCammon, J. A.; Karplus, M. Dynamical theory of activated processes in globular proteins. *Proc. Natl. Acad. Sci. U.S.A.* **1982**, *79*, 4035–4039.

(62) Skerra, A.; Brickmann, J. Simulation of voltage-driven hydrated cation transport through narrow transmembrane channels. *Biophys. J.* **1987**, *51*, 977–983.

(63) Impey, R. W.; Madden, P. A.; McDonald, I. R. Hydration and mobility of ions in solution. *J. Phys. Chem.* **1983**, *87*, 5071–5083.

Analysis of the instantaneous force acting on Na^+ at the transition state shows that the barrier crossing is controlled by localized interactions. This is consistent with the observation that the water–channel cross-coupling forces contribute significantly to the time-dependent friction acting on Na^+ at the transition state. The strongly coupled forces are due predominantly to the two nearest water molecules and four carbonyl oxygens in direct contact with the Na^+ ion. Analysis based on the Grote–Hynes theory of barrier crossing[34] indicates that Na^+ is sensitive to non-Markovian dynamical effects at the transition state. In contrast to Na^+, component analysis of the time-dependent friction shows that dissipation of the K^+ movement is influenced predominantly by the full static friction of the water molecules present in the channel.

The translocation of Na^+ in the β-helix, and by extrapolation to the smaller ion Li^+, is an activated process with significant free energy barriers; it is also sensitive to non-Markovian effects and controlled by local interactions at the transition state. Larger ions such as K^+, and by extrapolation Rb^+ and Cs^+, diffuse more rapidly in the β-helix because the barriers are significantly smaller; their motions are limited by the static friction constant and the diffusion of water molecules. Based on this analysis, the stochastic Brownian dynamics model[8] is capable of capturing the essential features of the dynamics of K^+ and larger ions inside the gramicidin channel. However, a generalized Langevin equation, including non-Markovian effects, is required for Na^+ and smaller ions. Multiple barrier rate models are more realistic for Li^+ and Na^+ than for the larger ions. They can be useful to fit the experimental current–voltage relations as long as they are correctly interpreted to include dissipative effects. The gas-phase transition-state theory expressed in terms of Planck's constant h

$$k_{gas} = \frac{k_B T}{h} e^{-\Delta E^*/k_B T} \tag{31}$$

often used to extract activation energy barriers from experiments[9,16] does not include dissipative effects and is not valid for reactions in liquids.[2] For example, the activation energy ΔE^* extracted by use of eq 31 from the transition rate of the Na^+ by the full treatment ($2.3 \times 10^8\ s^{-1}$) gives a value of 6.1 kcal/mol, different by 1.6 kcal/mol from the actual activation energy (4.5 kcal/mol).

The calculated diffusion constant of Na^+ in the β-helix appears to be in good agreement with experiment but the values for water and K^+ ion are larger than the experimental estimate by about 1 order of magnitude. Experimentally the diffusion constants of Na^+, K^+, and water are within a factor of 4 while the calculated values differ by more than 2 orders of magnitude; i.e., Na^+ is in approximate agreement with experiments, and K^+ and water are too fast. Since the mechanisms of transport are found to be so different for Na^+ versus K^+ and water, it is surprising that their experimental rates are so similar. The transport of K^+ is mostly controlled by the diffusion of water molecules in the channel, so it is not surprising that they are similar. That they are both overestimated in the β-helix simulations indicates that interactions with the pore, in the absence of ends effects, do not give rise to free energy barriers and dissipative effects that are sufficient to account for their mobilities. This finding suggests that other factors (i.e., the nonhomogeneous nature of the channel) must be responsible for the slow diffusion of water and K^+ through the gramicidin channel.

Molecular dynamics studies of a detailed atomic model of a gramicidin-like β-helix have revealed that transport of Na^+ and K^+ ions are influenced by different factors. It was shown previously that both water and channel forces contributed significantly to the potential of mean force of Na^+ while only the water forces controlled that of K^+.[1] The present analysis shows that the same microscopic factors govern the dynamics of Na^+ and K^+; for Na^+ both the channel and water forces are important while for K^+ it is the water alone. Further studies will focus on water mobility and the activation energy at the entrance and exit of a complete model for the gramicidin channel.[57]

Acknowledgment. Most of the calculations were done at the Pittsburgh Supercomputing Center. This work was supported in part by a grant from the National Science Foundation. Helpful discussions with John Straub, David Busath, and Olaf S. Andersen are gratefully acknowledged.

Registry No. K^+, 7440-09-7; Na^+, 7440-23-5; H_2O, 7732-18-5; gramicidin, 1405-97-6; poly(L,D)-alanine, 25281-63-4.

(64) Hladky, S. B.; Haydon, D. A. Ion transfer across lipid membranes in the presence of gramicidin A. *Biochim. Biophys. Acta* **1972**, *274*, 294–312.
(65) Wolynes, P. G. Dynamics of Electrolyte Solutions. *Annu. Rev. Phys. Chem.* **1980**, *31*, 345–376.